University of Nebraska - Lincoln
DigitalCommons@University of Nebraska - Lincoln

Papers from the Nebraska Center for Biotechnology

Biotechnology, Center for

9-13-2017

Cross-species complementation reveals conserved functions for EARLY FLOWERING 3 between monocots and dicots

He Huang

Malia A. Gehan

Sarah E. Huss

Sohpie Alvarez

Cesar Lizarraga

See next page for additional authors

Follow this and additional works at: https://digitalcommons.unl.edu/biotechpapers

 Part of the Biotechnology Commons, and the Molecular, Cellular, and Tissue Engineering Commons

This Article is brought to you for free and open access by the Biotechnology, Center for at DigitalCommons@University of Nebraska - Lincoln. It has been accepted for inclusion in Papers from the Nebraska Center for Biotechnology by an authorized administrator of DigitalCommons@University of Nebraska - Lincoln.

Authors

He Huang, Malia A. Gehan, Sarah E. Huss, Sohpie Alvarez, Cesar Lizarraga, Ellen L. Gruebbling, John Gierer, Michael J. Naldrett, Rebacca K. Bindbeutel, Bradley S. Evans, Todd C. Mockler, and Dmitri A. Nusinow

Received: 24 May 2017 | Revised: 10 August 2017 | Accepted: 13 September 2017

DOI: 10.1002/pld3.18

ORIGINAL RESEARCH

Cross-species complementation reveals conserved functions for EARLY FLOWERING 3 between monocots and dicots

He Huang[1] | Malia A. Gehan[1] | Sarah E. Huss[2] | Sophie Alvarez[1] | Cesar Lizarraga[1] | Ellen L. Gruebbling[3] | John Gierer[1] | Michael J. Naldrett[1] | Rebecca K. Bindbeutel[1] | Bradley S. Evans[1] | Todd C. Mockler[1] | Dmitri A. Nusinow[1]

[1]Donald Danforth Plant Science Center, St. Louis, MO, USA

[2]Webster University, Webster Groves, MO, USA

[3]Saint Louis University, St. Louis, MO, USA

Correspondence
Dmitri A. Nusinow, Donald Danforth Plant Science Center, St. Louis, MO, USA.
Email: meter@danforthcenter.org

Present address
Sophie Alvarez and Michael J. Naldrett, University of Nebraska-Lincoln, Lincoln, NE, USA.

Funding information
This work was supported by the National Science Foundation (NSF) grant (IOS-1456796) to D.A.N., the NSF (DBI-0922879) grant for acquisition of the LTQ-Velos Pro Orbitrap LC-MS/MS, the U.S. Department of Energy grants (DE-SC0006627, DE-SC0012639, and DE-SC0008769) to T.C.M., and the NSF-Plant Genome grant (IOS-1202682) to M.A.G.

Abstract

Plant responses to the environment are shaped by external stimuli and internal signaling pathways. In both the model plant *Arabidopsis thaliana* (*Arabidopsis*) and crop species, circadian clock factors are critical for growth, flowering, and circadian rhythms. Outside of *Arabidopsis*, however, little is known about the molecular function of clock gene products. Therefore, we sought to compare the function of *Brachypodium distachyon* (*Brachypodium*) and *Setaria viridis* (*Setaria*) orthologs of *EARLY FLOWERING 3*, a key clock gene in *Arabidopsis*. To identify both cycling genes and putative *ELF3* functional orthologs in *Setaria*, a circadian RNA-seq dataset and online query tool (Diel Explorer) were generated to explore expression profiles of *Setaria* genes under circadian conditions. The function of *ELF3* orthologs from *Arabidopsis*, *Brachypodium*, and *Setaria* was tested for complementation of an *elf3* mutation in *Arabidopsis*. We find that both monocot orthologs were capable of rescuing hypocotyl elongation, flowering time, and arrhythmic clock phenotypes. Using affinity purification and mass spectrometry, our data indicate that BdELF3 and SvELF3 could be integrated into similar complexes *in vivo* as AtELF3. Thus, we find that, despite 180 million years of separation, *BdELF3* and *SvELF3* can functionally complement loss of *ELF3* at the molecular and physiological level.

KEYWORDS
circadian clock, circadian RNA-seq, ELF3, flowering, growth, Setaria

1 | INTRODUCTION

Plants have developed sophisticated signaling networks to survive and thrive in diverse environments. Many plant responses are shaped, in part, by an internal timing mechanism known as the circadian clock, which allows for the coordination and anticipation of daily and seasonal variation in the environment (Greenham & McClung, 2015). Circadian clocks, which are endogenous oscillators with a period of approximately 24 hr, are critical for regulating the timing of physiology, development, and metabolism in all domains of life (Bell-Pedersen et al., 2005; Doherty & Kay, 2010; Edgar et al., 2012; Harmer, 2009; Wijnen & Young, 2006). In plants and blue-green algae, circadian clocks provide an experimentally observable adaptive advantage by synchronizing internal physiology with external environmental cues (Dodd et al., 2005; Green, Tingay, Wang, & Tobin, 2002; Ouyang, Andersson, Kondo, Golden, & Johnson, 1998; Rubin et al., 2017; Woelfle, Ouyang, Phanvijhitsiri, & Johnson,

This manuscript was previously deposited as a preprint at doi: (https://doi.org/10.1101/131185).

This is an open access article under the terms of the Creative Commons Attribution License, which permits use, distribution and reproduction in any medium, provided the original work is properly cited.
© 2017 The Authors. *Plant Direct* published by American Society of Plant Biologists, Society for Experimental Biology and John Wiley & Sons Ltd.

2004). Currently, circadian oscillators are best understood in the reference plant *Arabidopsis*, in which dozens of clock or clock-associated components have been identified using genetic screens and noninvasive, luciferase-based oscillating reporters (Hsu & Harmer, 2014; Nagel & Kay, 2012). These morning-, afternoon-, and evening-phased clock oscillators form multiple interconnected transcription–translation feedback loops and compose a complex network (Hsu & Harmer, 2014; Pokhilko et al., 2012). The *Arabidopsis* circadian clock regulates a significant portion of physiology, including photosynthesis, growth, disease resistance, starch metabolism, and phytohormone pathways (Covington, Maloof, Straume, Kay, & Harmer, 2008; Graf, Schlereth, Stitt, & Smith, 2010; Harmer et al., 2000; Michael, Mockler, Breton, Mcentee, & Byer, 2008; Wang, Barnaby, et al., 2011), with up to 30% of gene expression under circadian control (Covington et al., 2008; Michael et al., 2008).

Within the Arabidopsis clock network, a tripartite protein complex called the evening complex (EC) is an essential component of the evening transcription loop (Huang & Nusinow, 2016b). The EC consists of three distinct proteins, EARLY FLOWERING 3 (ELF3), EARLY FLOWERING 4 (ELF4), and LUX ARRHYTHMO (LUX, also known as PHYTOCLOCK1), with transcript and protein levels peaking in the evening (Doyle et al., 2002; Hazen et al., 2005; Hicks, Albertson, & Wagner, 2001; Nusinow et al., 2011; Onai & Ishiura, 2005). The EC plays a critical role in maintaining circadian rhythms, by repressing expression of key clock genes (Dixon et al., 2011; Helfer et al., 2011; Herrero et al., 2012; Kolmos et al., 2011; Mizuno et al., 2014). Loss-of-function mutation of any EC component in *Arabidopsis* results in arrhythmicity of the circadian clock and causes excessive cellular elongation and early flowering regardless of environmental photoperiod (Doyle et al., 2002; Hazen et al., 2005; Hicks et al., 2001; Khanna, Kikis, & Quail, 2003; Kim, Hicks, & Somers, 2005; Nozue et al., 2007; Nusinow et al., 2011; Onai & Ishiura, 2005).

In *Arabidopsis*, ELF3 directly interacts with ELF4 and LUX, functioning as a scaffold to bring ELF4 and LUX together (Herrero et al., 2012; Nusinow et al., 2011). Additional protein–protein interaction studies and tandem affinity purification coupled with mass spectrometry (AP-MS) have identified many ELF3-associating proteins and established ELF3 as a hub of a complex protein–protein interaction network, which consists of key components from the circadian clock pathway and light signaling pathways (Huang & Nusinow, 2016b; Huang, Alvarez, Bindbeutel, et al., 2016; Liu, Covington, Fankhauser, Chory, & Wagner, 2001; Yu et al., 2008). In this network, ELF3 directly interacts with the major red light photoreceptor phytochrome B (phyB), and CONSTITUTIVE PHOTOMORPHOGENIC 1 (COP1), which is an E3 ubiquitin ligase required for proper regulation of photomorphogenesis and also interacts with phyB (Liu et al., 2001; Yu et al., 2008). The physical interaction among ELF3, phyB, and COP1, together with recruitment of direct interacting proteins to the network, provides biochemical evidence for cross talk between circadian clock and light signaling pathways (Huang & Nusinow, 2016b). Although much work does translate from *Arabidopsis* to other plant species, interaction between ELF3 and other proteins has yet to be tested in species outside *Arabidopsis*. Whether evening complex-like protein assemblages or a similar ELF3-containing protein-protein interaction network exists in species outside *Arabidopsis* is an interesting question to ask.

Identification and characterization of clock genes in diverse plant species have revealed that many clock components are broadly conserved (Filichkin et al., 2011; Khan, Rowe, & Harmon, 2010; Lou et al., 2012; Song, Ito, & Imaizumi, 2010). Furthermore, comparative genomics analysis has found that circadian clock components are selectively retained after genome duplication events, suggestive of the importance of their role in maintaining fitness (Lou et al., 2012). Recently, mutant alleles of *ELF3* were identified associated with the selection of favorable photoperiodism phenotypes in several crops, such as pea (*Pisum sativum*), rice (*Oryza sativa*), soybean (*Glycine max*), and barley (*Hordeum vulgare* L.) (Faure et al., 2012; Lu et al., 2017; Matsubara et al., 2012; Saito et al., 2012; Weller et al., 2012; Zakhrabekova et al., 2012). These findings are consistent with the reported functions of *Arabidopsis* ELF3 in regulating the photoperiodic control of growth and flowering (Hicks et al., 2001; Huang & Nusinow, 2016b; Nozue et al., 2007; Nusinow et al., 2011). However, opposed to the early flowering phenotype caused by *elf3* mutants in *Arabidopsis*, pea, and barley (Faure et al., 2012; Hicks et al., 2001; Weller et al., 2012), loss-of-function mutation of the rice or soybean *ELF3* ortholog results in delayed flowering (Lu et al., 2017; Saito et al., 2012), suggesting ELF3-mediated regulation of flowering varies in different plant species. The molecular mechanisms underlying this difference have not been thoroughly elucidated.

Brachypodium distachyon is a C3 model grass closely related to wheat (*Triticum aestivum*), barley, oats (*Avena sativa*), and rice. *Setaria viridis* is a C4 model grass closely related to maize (*Zea mays*), sorghum (*Sorghum bicolor*), sugarcane (*Saccharum officinarum*), and other bioenergy grasses. Both grasses are small, transformable, rapid-cycling plants with recently sequenced genomes, making them ideal model monocots for comparative analysis with *Arabidopsis* (Bennetzen et al., 2012; Brutnell et al., 2010). Computational analysis of *Brachypodium* has identified putative circadian clock orthologs (Higgins, Bailey, & Laurie, 2010), including *BdELF3*. However, no such comparative analysis has been carried out systematically in *Setaria* to identify putative orthologs of circadian clock genes. Therefore, we generated a RNA-seq time-course dataset to analyze the circadian transcriptome of *Setaria* after either photo- or thermo-entrainment and developed an online gene-expression query tool (Diel Explorer) for the community. We found that the magnitude of circadian-regulated genes in *Setaria* is similar to other monocots after photo-entrainment, but much less after thermal entrainment. We further analyzed the functional conservation of *SvELF3*, together with previously reported *BdELF3*, by introducing both *ELF3* orthologs into *Arabidopsis elf3* mutant for physiological and biochemical characterization. We found that *Brachypodium* and *Setaria ELF3* can complement the hypocotyl elongation, flowering time and circadian arrhythmia phenotypes caused by the *elf3* mutation in *Arabidopsis*. Furthermore, AP-MS analyses found that *Brachypodium* and *Setaria* ELF3 were integrated into a similar protein–protein interaction network *in vivo* as their *Arabidopsis* counterpart. Our data collectively demonstrated the functional conservation of ELF3 among *Arabidopsis*, *Brachypodium*, and *Setaria* are likely due to

the association with same protein partners, providing insights of how ELF3 orthologs potentially function in grasses.

2 | METHODS

2.1 | Plant materials and growth conditions

For *Arabidopsis*, wild-type (Columbia-0) and *elf3-2* plants carrying the CCA1::LUC reporter were described previously (Nusinow et al., 2011; Pruneda-Paz, Breton, Para, & Kay, 2009). Seeds were surface sterilized and plated on 1/2× Murashige and Skoog (MS) basal salt medium with 0.8% agar + 1% (w/v) sucrose. After 3 days of stratification, plates were placed horizontally in a Percival incubator (Percival Scientific, Perry, IA), supplied with 80 μmol m^{-2} s^{-1} white light and set to a constant temperature of 22°C. Plants were grown under 12-h light/12-h dark cycles (12L:12D) for 4 days (for physiological experiments) or for 10 days (for AP-MS) before assays.

For *Setaria* circadian expression profiling by RNA-seq, seeds were stratified for 5 days at 4°C before being moved to entrainment conditions. Plants were grown under either LDHH or LLHC (L: light, D: dark, H: hot, C: cold) entrainment condition, and then sampled for RNA-seq in constant light and constant temperature (32°C) conditions (F, for free-running) every 2 hr for 48 hr. Light intensity was set to 400 μmol m^{-2} s^{-1} white light. In LDHH-F, stratified *Setaria* seeds were grown for 10 days under 12L:12D and constant temperature (32°C) before sampling in constant light and constant temperature. In LLHC-F, stratified *Setaria* seeds were grown for 10 days under constant light conditions and cycling temperature conditions 12 h at 32°C (subjective day)/12 h at 22°C (subjective night) before sampling in constant conditions. Two experimental replicates were collected for each entrainment condition.

2.2 | Setaria circadian RNA-seq

The second leaf from the top of seventeen *S. viridis* plants was selected for RNA-seq sampling at each time point for each sampling condition. Five replicate samples were pooled after being ground in liquid nitrogen and resuspended in lithium chloride lysis binding buffer (Wang, Si, et al., 2011). RNA-seq libraries from leaf samples were constructed according to the previous literature (Wang, Si, et al., 2011) with one major modification. Rather than extracting RNA then mRNA from ground leaf samples (Wang, Si, et al., 2011), mRNA was extracted directly from frozen ground leaf samples similar to the method described in Kumar et al. (2012), except that two additional rounds of wash, binding, and elution steps after treatment with EDTA were necessary to remove rRNA from samples. mRNA quantity was assessed using a Qubit with a Qubit RNA HS Kit, and mRNA quality was assessed using a Bioanalyzer and Plant RNA PiCO chip. Ninety-six library samples were multiplexed 12 per lane, for a total of eight lanes of Illumina Hiseq 2000 sequencing. Paired-end 101-bp sequencing was carried out at MOgene (St. Louis, MO). Raw data and processed data can be found on NCBI's Gene Expression Omnibus (GEO; (Barrett et al., 2013; Edgar, Domrachev, & Lash, 2002)) and are accessible with identification number GSE97739 (https://www.ncbi.nlm.nih.gov/geo/query/acc.cgi?acc=GSE97739).

RNA-seq data were trimmed with BBTools (v36.20) using parameters: ktrim=r k=23 mink=11 hdist=1 tpe tbo ktrim=l k=23 mink=11 hdist=1 tpe tbo qtrim=rl trimq=20 minlen=20 (Bushnell, 2016). Any parameters not specified were run as default. Before trimming, we had 1,814,939,650 reads with a mean of 18,905,621 reads per sample and a standard deviation of 2,875,187. After trimming, we have 1,646,019,593 reads with a mean of 17,146,037 reads per sample and a standard deviation of 2,411,061. Kallisto (v 0.42.4; (Bray, Pimentel, Melsted, & Pachter, 2016)) was used to index the transcripts with the default parameters and the *S. viridis* transcripts fasta file (Sviridis_311_v1.1) from Phytozome (Goodstein et al., 2012). The reads were quantified with parameters:-t 40 -b 100. Any parameters not specified were run as default. Kallisto output was formatted for compatibility with JTK-Cycle (v3.1; (Hughes, Hogenesch, & Kornacker, 2010)), and circadian cycles were detected. To query the *Setaria* expression data, we developed Diel Explorer. The tool can be found at http://shiny.bioinformatics.danforthcenter.org/diel-explorer/. Underlying code for Diel Explorer is available on Github (https://github.com/danforthcenter/diel-explorer).

2.3 | Plasmid constructs and generation of transgenic plants

Coding sequences (without the stop codon) of *AtELF3* (*AT2G25930*) and *SvELF3a* (*Sevir.5G206400.1*) were cloned into the pENTR/D-TOPO vector (ThermoFisher Scientific, Waltham, MA), verified by sequencing, and were recombined into the pB7HFC vector (Huang, Alvarez, Bindbeutel, et al., 2016) using LR Clonease (ThermoFisher Scientific). Coding sequence of *BdELF3* (*Bradi2g14290.1*) was submitted to the U.S. Department of Energy Joint Genome Institute (DOE-JGI), synthesized by the DNA Synthesis Science group, and cloned into the pENTR/D-TOPO vector. Sequence validated clones were then recombined into pB7HFC as described above. The pB7HFC-At/Bd/SvELF3 constructs were then transformed into *elf3-2* [*CCA1::LUC*] plants by the floral dip method (Zhang, Henriques, Lin, Niu, & Chua, 2006). Homozygous transgenic plants were validated by testing luciferase bioluminescence, drug resistance, and by PCR-based genotyping. All primers used in this article were listed in Table S1.

2.4 | Hypocotyl and flowering time measurement

Twenty seedlings of each genotype were arrayed and photographed with a ruler for measuring hypocotyl length using the ImageJ software (NIH) (Schneider, Rasband, & Eliceiri, 2012). The procedure was repeated three times. For measuring flowering time, 12 plants of each genotype were placed in a random order and were grown under the long-day condition (light:dark = 16:8 hr). The seedlings were then observed every day at 12:00 PM; the date on which each seedling began flowering, indicated by the growth of a ~1 cm inflorescence stem, was recorded along with the number of rosette leaves produced up to that date. ANOVA with Bonferroni correction

was measured using GraphPad Prism version 6.00 (GraphPad Software, La Jolla California USA, www.graphpad.com).

2.5 | Circadian assays in *Arabidopsis*

Seedlings were transferred to fresh 1/2× MS plates after 5 days of entrainment under the 12L:12D condition and sprayed with sterile 5 mM luciferin (Gold Biotechnology, St. Louis, MO) prepared in 0.1% (v/v) Triton X-100 solution. Sprayed seedlings were then imaged in constant light (70 μmol m^{-2} sec^{-1}, wavelengths 400, 430, 450, 530, 630, and 660 set at intensity 350 (Heliospectra LED lights, Göteborg, Sweden)). Bioluminescence was recorded after a 120–180s delay to diminish delayed fluorescence (Gould et al., 2009) over 5 days using an ultra-cooled CCD camera (Pixis 1024B, Princeton Instruments) driven by Micro-Manager software (Edelstein, Amodaj, Hoover, Vale, & Stuurman, 2010; Edelstein et al., 2014). The images were processed in stacks by Metamorph software (Molecular Devices, Sunnyvale, CA), and rhythms determined by fast Fourier-transformed nonlinear least squares (FFT-NLLS) (Plautz et al., 1997) after background subtraction using the interface provided by the Biological Rhythms Analysis Software System 3.0 (BRASS) available at http://www.amillar.org.

2.6 | Yeast two-hybrid analysis

Yeast two-hybrid assays were carried out as previously described (Huang, Alvarez, Bindbeutel, et al., 2016). In brief, the DNA binding domain (DBD) or activating domain (AD)-fused constructs were transformed using the Li-Ac transformation protocol (Clontech) into *Saccharomyces cerevisiae* strain Y187 (MATα) and the AH109 (MATa), respectively. Two strains of yeast were then mated to generate diploid with both DBD and AD constructs. Protein–protein interaction was tested in diploid yeast by replica plating on CSM –Leu –Trp –His media supplemented with extra adenine (30 mg/L final concentration) and 2 mM 3-amino-1,2,4-triazole (3AT). Pictures were taken after 4-day incubation at 30°C. All primers used for cloning plasmid constructs were listed in Table S1.

2.7 | Protein extraction and western blotting

Protein extracts were made from 10-day-old seedlings as previously described (Huang, Alvarez, Bindbeutel, et al., 2016) and loaded 50 μg to run 10% SDS-PAGE. For Western blots, all of the following primary and secondary antibodies were diluted into PBS + 0.1% Tween and incubated at room temperature for 1 hr: anti-FLAG®M2-HRP (Sigma, A8592, diluted at 1:10,000) and anti-Rpt5-rabbit (ENZO Life Science, BML-PW8245-0025, diluted at 1:5000), and anti-rabbit-HRP secondary antibodies (Sigma, A0545, diluted at 1:10,000).

2.8 | Affinity purification and mass spectrometry (AP-MS)

Protein extraction methods and protocols for AP-MS were described previously (Huang, Alvarez, & Nusinow, 2016; Huang & Nusinow, 2016a; Huang, Alvarez, Bindbeutel, et al., 2016; Huang, Yoo, et al., 2016). In brief, transgenic seedlings carrying the At/Bd/SvELF3-HFC constructs were grown under 12L:12D conditions for 10 days and were harvested at dusk (ZT12). Five grams of seedlings was needed per replicate to make protein extracts, which underwent tandem affinity purification utilizing the FLAG and His epitopes of the fusion protein. Purified samples were reduced, alkylated, and digested by trypsin. The tryptic peptides were then injected to an LTQ-Orbitrap Velos Pro (ThermoFisher Scientific) coupled with a U3000 RSLCnano HPLC (ThermoFisher Scientific) with settings described previously (Huang, Alvarez, Bindbeutel, et al., 2016).

2.9 | AP-MS data analysis

Data analysis was carried out as previously described (Huang, Alvarez, Bindbeutel, et al., 2016). The databases searched were TAIR10 database (20101214, 35,386 entries) and the cRAP database (http://www.thegpm.org/cRAP/). Peptide identifications were accepted if they could be established at greater than 95.0% probability and the Scaffold Local FDR was <1%. Protein identifications were accepted if they could be established at greater than 99.0% probability as assigned by the Protein Prophet algorithm (Keller, Nesvizhskii, Kolker, & Aebersold, 2002; Nesvizhskii, Keller, Kolker, & Aebersold, 2003). A full list of all identified proteins (reporting total/exclusive unique peptide count and percent coverage) can be found in Table S2. The mass spectrometry proteomics data have been deposited to the ProteomeXchange Consortium (Vizcaino et al., 2014) via the PRIDE partner repository with the dataset identifier PXD006352 and https://doi.org/10.6019/PXD006352.

2.10 | Accession numbers

AtELF3 (AT2G25930), *BdELF3* (*Bradi2g14290.1*), *SvELF3a* (*Sevir.5G206400.1*) and *SvELF3b* (*Sevir.3G123200.1*) are used in this article. Accession numbers for all the At/Bd/Sv/ELF3-associated proteins can be found in Table 1 and Table S2.

3 | RESULTS

3.1 | Identifying and cloning *ELF3* orthologs from *Brachypodium* and *Setaria*

ELF3 is a plant-specific nuclear protein with conserved roles in flowering and the circadian clock in multiple plant species (Faure et al., 2012; Herrero et al., 2012; Liu et al., 2001; Lu et al., 2017; Matsubara et al., 2012; Saito et al., 2012; Weller et al., 2012; Zakhrabekova et al., 2012). To identify ELF3 orthologs in monocots, we used the protein sequence of *Arabidopsis* ELF3 (AtELF3) to search the proteomes of two model monocots *Brachypodium* and *Setaria* using BLAST (Altschul, Gish, Miller, Myers, & Lipman, 1990). Among the top hits, we identified a previously reported *ELF3* homolog in *Brachypodium* (*Bradi2g14290.1*, *BdELF3*) (Calixto, Waugh, & Brown, 2015; Higgins et al., 2010) and two putative *ELF3* homologous genes *Sevir.5G206400.1* (referred as *SvELF3a*) and *Sevir.3G123200.1*

(referred as *SvELF3b*) in *Setaria*. We used Clustal Omega (http://www.ebi.ac.uk/Tools/msa/clustalo/) to conduct multiple sequence alignments of comparing protein sequences of *ELF3* orthologs with that of *AtELF3* (Sievers et al., 2011). *BdELF3*, *SvELF3a*, and *SvELF3b* encode proteins with similar identity compared to *AtELF3* (34.7–36.8%) (Fig. S1). When compared to *BdELF3*, *SvELF3b* was 74.3% identical while *SvELF3a* was 57.4% identical (Fig. S1). Therefore, to maximize the diversity of ELF3 sequences used in this study, we cloned full-length cDNAs encoding BdELF3 and SvELF3a.

3.2 | Diel explorer of *Setaria* circadian data

In Arabidopsis, ELF3 cycles under diel and circadian conditions (constant condition after entrainment) with a peak phase in the evening (Covington et al., 2001; Hicks et al., 2001; Nusinow et al., 2011). We queried an available diurnal time-course expression dataset for *Brachypodium* from the DIURNAL website and found that *BdELF3* expression cycles under diel conditions (LDHH, 12-h light/12-h dark cycles with constant temperature, Fig. S2a), but not under circadian conditions in available data (LDHC-F or LDHH-F, Fig. S2b) (Filichkin et al., 2011; Mockler et al., 2007). Also different from *AtELF3*, transcript levels of *BdELF3* accumulate at dawn rather than peak in the evening (Fig. S2a) when grown under diel conditions, suggesting different regulations on *ELF3* expression between monocot and dicot plants. Neither diel nor circadian expression data for *Setaria* were available. Therefore, we generated RNA-seq time-course data to examine *SvELF3* expression as well as the circadian expression of other clock orthologs after both photocycle and thermocycle entrainment. In addition, we developed the Diel Explorer tool (http://shiny.bioinformatics.danforthcenter.org/diel-explorer/) to query and visualize *Setaria* circadian-regulated gene expression (Fig. S3). 48,594 *Setaria* transcripts are represented in the two datasets entrained under either photocycles (LDHH-F) or thermocycles (LLHC-F). With Diel Explorer, users can manually enter a list of transcript identifiers, gene ontology (GO) terms, or gene orthologs, plot gene expression, and download data. Alternatively, users can upload files of transcript identifiers or gene orthologs, and/or filter the datasets by entrainment, phase, or significance cutoffs. Data and graphs can be downloaded directly using Diel Explorer. The tool serves as a community resource that can be expanded to include other circadian or diurnal data in the future. The underlying code is available on Github (https://github.com/danforthcenter/diel-explorer).

For our analysis, JTK-Cycle was used to detect cycling *Setaria* genes at cutoff that had a false-positive rate of 0 with simulated data (Bonferroni-adjusted p-value < .001) (Hughes et al., 2010). Under photoperiod entrainment (LDHH-F), 5,585 of the 48,594 *Setaria* transcripts are circadian-regulated (Bonferroni-adjusted p-value < .001). This proportion of photoperiod-entrained circadian genes (~11.5%) is similar to maize (10.8%), rice (12.6%), and poplar (11.2%) data sets, but much smaller than the approximately 30% reported for *Arabidopsis* (Covington et al., 2008; Filichkin et al., 2011; Khan et al., 2010). Under thermocycle entrainment (LLHC-F), 582 of the 48,594 *Setaria* transcripts are circadian-regulated (Bonferroni-adjusted p-value < .001). Therefore, only ~1.2% of *Setaria* transcripts are circadian cycling under thermocycle entrainment. The ~10-fold reduction in circadian cycling genes between photocycle and thermocycle entrainment (Fig. S4) is interesting considering that there was less than 1% difference in the number of genes with a circadian period between photocycle and thermocycle entrainment in C3 monocot rice (*Oryza japonica*) (Filichkin et al., 2011). The reduction in cycling genes between the two entrainment conditions in *Setaria* compared to rice is an indication that circadian regulation could vary greatly among monocots. Also, the difference in number of cycling genes between monocots and dicots may represent a significant reduction of the role of the circadian clock between these lineages. Wang et al., 2014 found that different metabolites peak along a leaf developmental gradient (Wang et al., 2014) and when we query that expression dataset on Maize eFG browser (Li et al., 2010) for expression of clock genes GRMZM2G175265 and GRMZM2G014902 (zmCCA1), there is an increasing gradient of absolute expression from base to tip. If developmental zones were asynchronous, the overall reduction in cycling genes between monocots and dicots would indicate a stronger role of developmental gradients in modulating the monocot circadian clock along with environment. However, gradients in expression of clock genes are not necessarily evidence that developmental zones are asynchronous, as that gradient could also result in reduction in cycling gene amplitude between developmental zones, but not asynchronicity. Therefore, to examine whether the overall reduction in cycling genes is due to asynchronicity between developmental zones, a circadian time-course along development would be necessary.

In addition to the overall reduction in circadian genes, the phase with the most number of cycling genes was ZT18 after light entrainment (LDHH-F; Fig. S4), but ZT12 with temperature entrainment (LLHC-F; Fig. S4), which is consistent with previous studies that have found significant differences in temperature and light entrainment of the circadian clock (Boikoglou et al., 2011; Michael, Salome, & McClung, 2003; Michael et al., 2008). There are 269 genes that are considered circadian-regulated and are cycling under both LDHH-F and LLHC-F conditions (Bonferroni-adjusted p-value < .001). The list of 269 genes that overlap between photocycle and thermocycle entrainment includes best matches for Arabidopsis core clock components *TIMING OF CAB EXPRESSION 1* (*TOC1*, *AT5G61380.1*; *Sevir.1G241000.1*), *LATE ELONGATED HYPOCOTYL* (*LHY*, *AT1G01060*; *Sevir.6G053100.1*), and *CCA1*-like gene *REVEILLE1* (*RVE1*, *AT5G17300.1*; *Sevir.1G280700.1*). However, putative *Setaria* orthologs of *TOC1*, *LHY*, and *RVE1* all have different circadian phases under LDHH entrainment compared to LLHC entrainment (Figure 1). In fact, the majority (233/269) of overlapping circadian genes in *Setaria* have a distinct circadian phase under thermocycle compared to photocycle entrainment (Fig. S4). We also found that putative orthologs of *PSEUDO-RESPONSE REGULATOR 7* (*PRR7*, *AT5G02810*; *Sevir.2G456400.1*; related to *OsPRR73* (Murakami, Ashikari, Miura, Yamashino, & Mizuno, 2003)) and *LUX ARRHYTHMO* (*LUX*, *AT3G46640*; *Sevir.5G474200.1*) cycle significantly under LDHH-F but not LLHC-F conditions (Figure 1). Neither

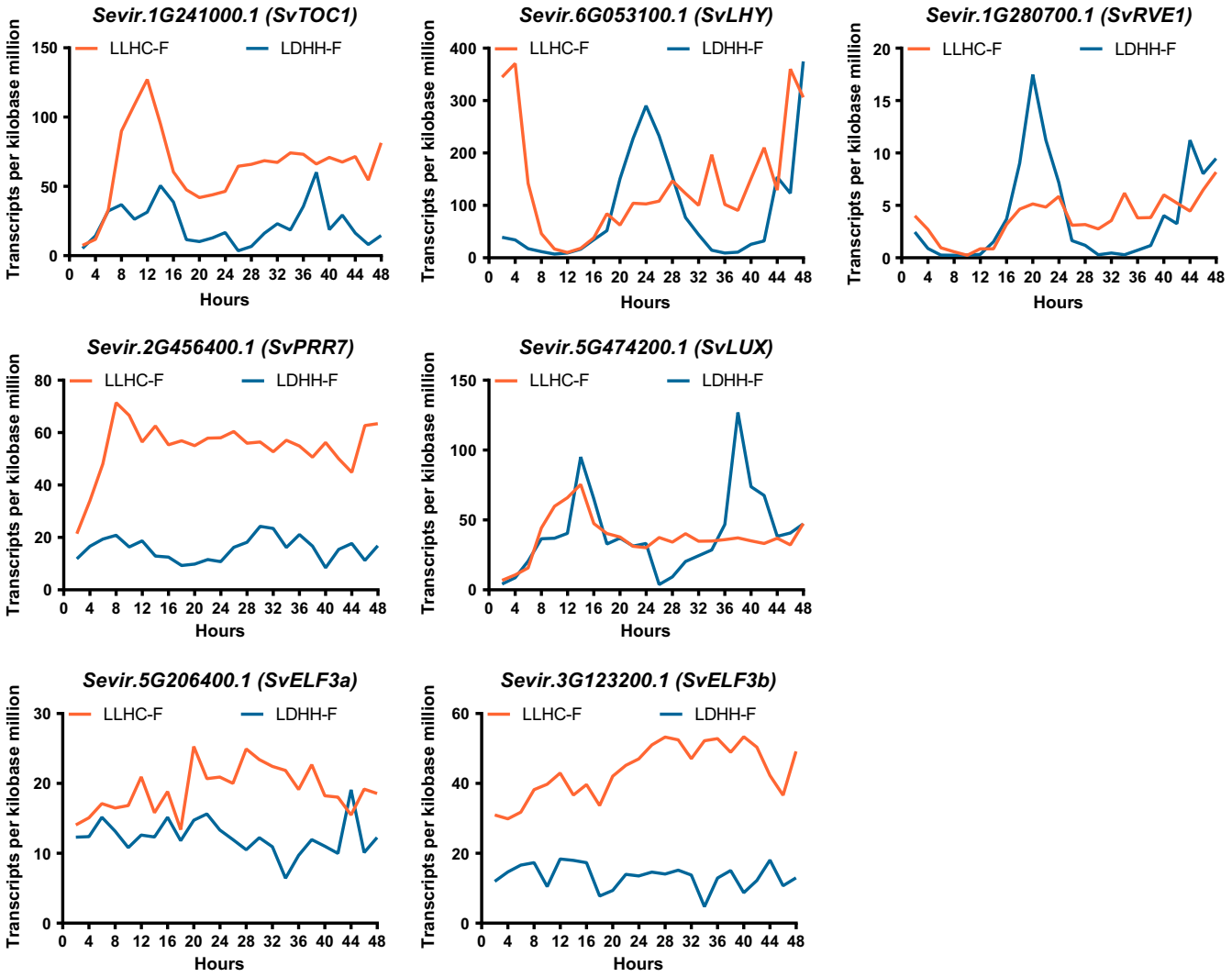

FIGURE 1 Circadian expression profiles of putative *Setaria* clock components from Diel Explorer using time-course RNA-seq data. *Setaria* plants were entrained by either photocycle (LDHH) or thermocycle (LLHC), followed by being sampled every 2 hr for 48 hr under constant temperature and light conditions (Free-Running; F) to generate time-course RNA-seq data. Mean values of transcripts per kilobase million (TPM) from two experimental replicates for each timepoints per gene were plotted

SvELF3a nor *SvELF3b* cycles under circadian conditions after photo- or thermo-entrainment (Figure 1), similar to *ELF3* orthologs in *Brachypodium* (Fig. S2) (Mockler et al., 2007) and rice (Filichkin et al., 2011). This is different from *AtELF3*, which continues to cycle under constant condition after either photo- or thermos-entrainment (Fig. S5) (Mockler et al., 2007). The difference in expression of these putative orthologs between *Arabidopsis* and monocots *Setaria*, *Brachypodium*, and rice suggests that the architecture of the circadian clock may have significant differences in response to environmental cues in these two species.

3.3 | BdELF3 and SvELF3 rescue growth and flowering defects in *Arabidopsis elf3* mutant

Although the circadian expression pattern of *Brachypodium ELF3* and *Setaria ELF3* is different from that of *Arabidopsis ELF3*, it is still possible that the *ELF3* orthologs have conserved biological functions. To test this, we sought to determine whether *BdELF3* or *SvELF3a* could complement the major phenotypic defects of the *elf3* mutant in *Arabidopsis*, namely hypocotyl elongation, time to flowering, or circadian rhythmicity. To this end, we constitutively expressed *BdELF3*, *SvELF3a* (hereafter referred as *SvELF3*), and *AtELF3* cDNAs by the *35S Cauliflower mosaic virus* promoter in the *Arabidopsis elf3-2* mutant expressing a *LUCIFERASE* reporter driven by the promoter of *CIRCADIAN CLOCK ASSOCIATED 1* (*CCA1*) (*elf3-2* [*CCA1:LUC*]) (Pruneda-Paz et al., 2009). All three ELF3 coding sequences were fused to a C-terminal His_6-3xFlag affinity tag (HFC), which enables detection by Western blotting and identification of protein-protein interaction by affinity purification and mass spectrometry (AP-MS) (Huang, Alvarez, Bindbeutel, et al., 2016). After transforming these constructs, we identified and selected two biologically independent transgenic lines with a single insertion of each At/Bd/SvELF3-HFC construct. Western blot analysis using FLAG antibodies detected the expression of all ELF3-HFC fusion proteins (Fig. S6).

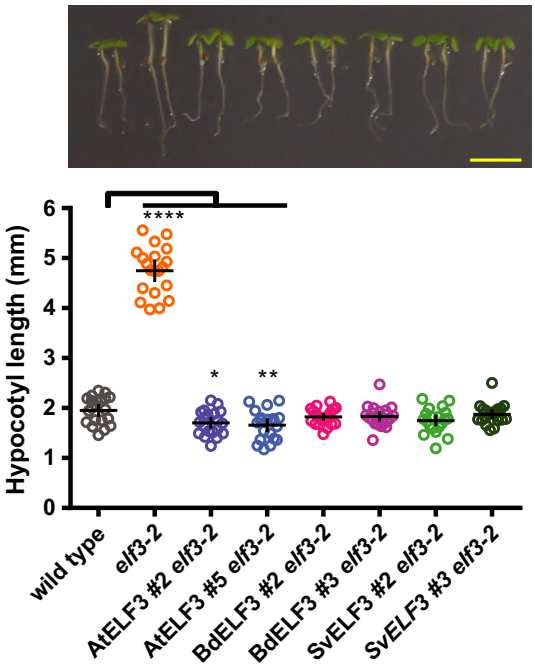

FIGURE 2 ELF3 orthologs suppress hypocotyl elongation defects in *elf3-2*. The hypocotyls of 20 seedlings of wild type, *elf3-2* mutant, AtELF3 *elf3-2*, BdELF3 *elf3-2*, and SvELF3 *elf3-2* (two independent transgenic lines for each ELF3 ortholog) were measured at 4 days after germination under 12-hr light:12-hr dark growth conditions at 22°C. Upper panel shows representative seedlings of each genotype, with scale bar equal to 5 mm. Mean and 95% confidence intervals are plotted as crosshairs. This experiment was repeated three times with similar results. ANOVA with Bonferroni correction was used to generate adjusted *p* values, * <.05, ** <.01, **** <.0001

Next, we asked whether expressing At/Bd/SvELF3-HFC fusion proteins could rescue the mutation defects caused by *elf3-2*. When plants are grown under light/dark cycles (12-hr light:12-hr dark), *elf3-2* mutant plants elongate their hypocotyls much more than wild-type plants (4.75 ± 0.48 mm vs. 1.95 ± 0.27 mm, respectively. ± = standard deviation) (Figure 2). The long hypocotyl defect in *elf3-2* was effectively suppressed by expressing either AtELF3, or ELF3 orthologs (BdELF3 *or* SvELF3) (Figure 2). These data show that the monocot ELF3 orthologs function similarly to *Arabidopsis* ELF3 in the regulation of hypocotyl elongation in seedlings.

In addition to regulating phenotypes in seedlings, ELF3 also functions in adult plants to suppress the floral transition. Loss of function in Arabidopsis ELF3 results in an early flowering phenotype regardless of day length (Hicks et al., 2001; Liu et al., 2001; Zagotta, Shannon, Jacobs, & Meeks-Wagner, 1992). To determine how monocot ELF3 orthologs compared to *Arabidopsis* ELF3 in flowering time regulation, we compared flowering responses under long-day conditions among wild-type, *elf3-2*, and *elf3-2* transgenic lines expressing AtELF3, BdELF3, or SvELF3 (At/Bd/SvELF3-HFC). Constitutive overexpression of AtELF3 led to a delay in flowering in long days (Figure 3) as previously observed (Liu et al., 2001). Similarly, constitutive expression of BdELF3 or SvELF3 caused plants to flower significantly later than the *elf3* mutants. These data show that all ELF3 orthologs can function to repress the rapid transition to flowering of the *elf3* mutation when constitutively expressed in adult plants.

3.4 | BdELF3 and SvELF3 restore the circadian rhythmicity in *Arabidopsis elf3* mutant

ELF3 is a key component of the *Arabidopsis* circadian clock and is critical for maintaining the periodicity and amplitude of rhythms as shown using the *CCA1* promoter-driven luciferase reporter (CCA:LUC) (Covington et al., 2001; Hicks et al., 1996; Nusinow et al., 2011). To determine whether BdELF3 or SvELF3 could rescue the arrhythmic phenotype of the *elf3* mutation, we analyzed the rhythms of the *CCA1::LUC* reporter under constant light conditions after diel entrainment (12-hr light: 12-hr dark at constant 22°C). Relative amplitude error (RAE) analysis found that 100% of wild type and nearly all of the three *elf3-2* transgenic lines expressing AtELF3, BdELF3 (BdELF3 *#3* was 87.5% rhythmic), and SvELF3 were rhythmic, while only 37.5% of the *elf3-2* lines had measurable rhythms (RAE < 0.5) (Fig. S7). Comparison of average period length found that the AtELF3 expressing lines completely rescued the period

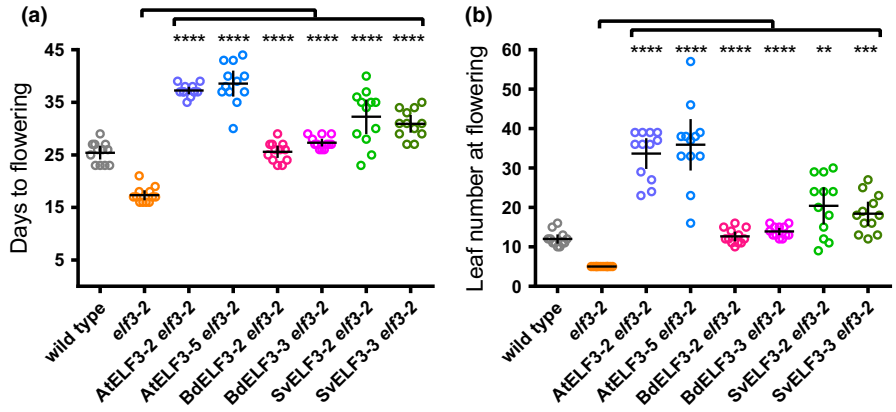

FIGURE 3 ELF3 orthologs suppress time to flowering of *elf3-2*. 12 wild-type, *elf3-2* mutant, AtELF3 *elf3-2*, BdELF3 *elf3-2*, and SvELF3 *elf3-2* seedlings from two independent transformations were measured for days (a) and number of rosette leaves (b) at flowering (1 cm inflorescence). Mean and 95% confidence intervals are plotted as crosshairs. This experiment was repeated twice with similar results. ANOVA with Bonferroni correction was used to generate adjusted *p* values, **<.01, ***<.001, ****<.0001, of measurements when compared to the *elf3-2* mutant line

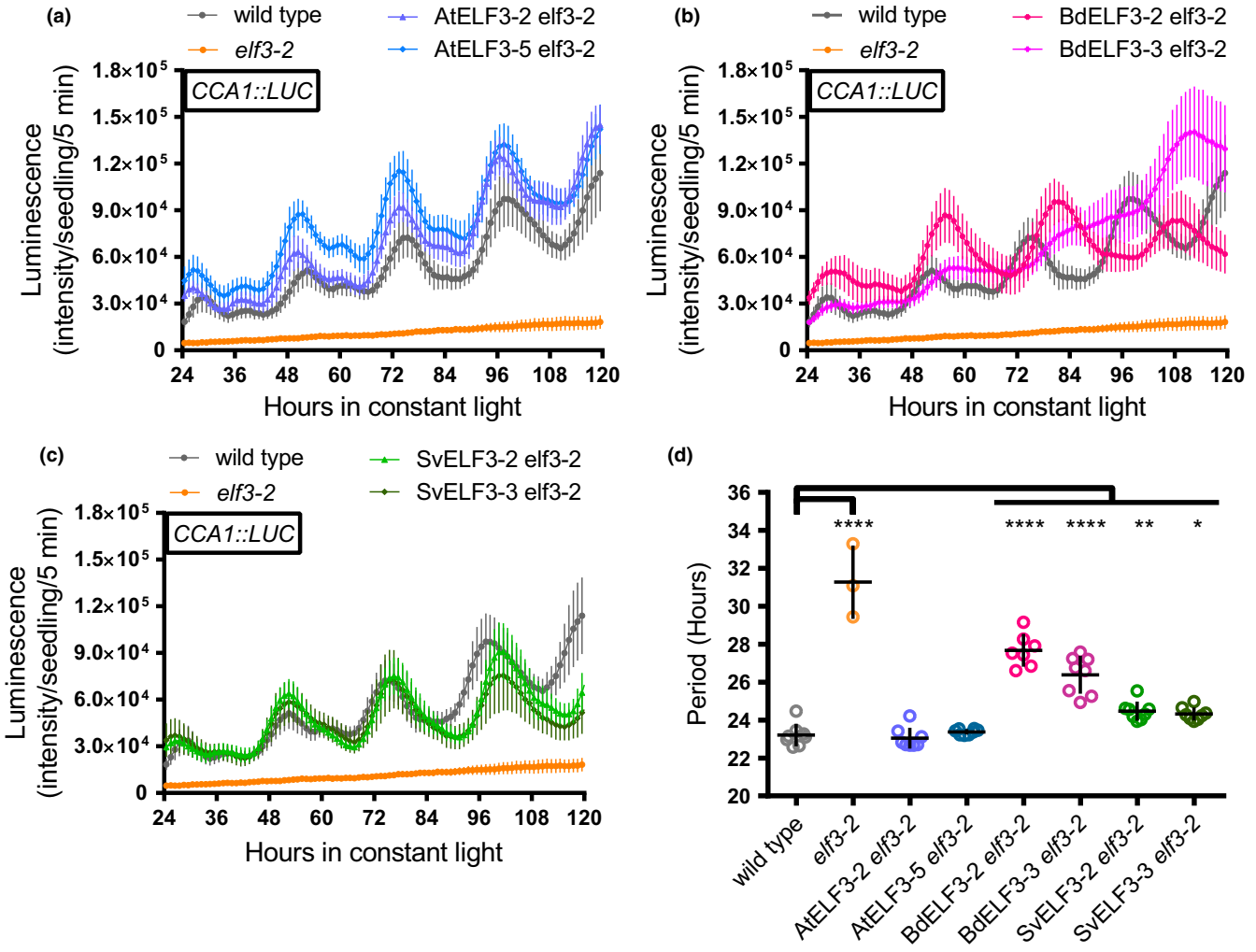

FIGURE 4 ELF3 orthologs can recover *CCA1::LUC* rhythms and amplitude in *elf3-2* mutants. Eight seedlings of wild type, *elf3-2* mutant, AtELF3 *elf3-2* (a), BdELF3 *elf3-2* (b), and SvELF3 *elf3-2* (c) from two independent transformations were imaged for bioluminescence under constant light after entrainment in 12-hr light:12-hr dark growth conditions at 22°C. Each plot shows average bioluminescence of all seedlings along with 95% confidence interval (error bars). This experiment was repeated four times with similar results. Note that wild-type and *elf3-2* mutant data were plotted on all graphs for comparison. (d) Periods of seedlings. Only periods with a relative amplitude error below 0.5 (see also Fig. S7) were plotted. Mean and 95% confidence intervals are plotted as crosshairs. ANOVA with Bonferroni correction was used to generate adjusted *p* values, * <.05, ** <.01, *** <.001, **** <.0001, of measurements when compared to the wild type

and amplitude defects in the *elf3* mutant (Figure 4a,d). The SvELF3 and BdELF3 lines also rescued the amplitude defect (Figure 4b,c), but their period was longer than wild type (compare 23.21 ± 0.59 hr for wild type to BdELF3 *#2* = 27.68 ± 0.86 hr, BdELF3 *#3* = 26.39 ± 1.01 hr, SvELF3 *#2* = 24.47 ± 0.50 hr, SvELF3 *#3* = 24.32 ± 0.34 hr, and *elf3-2* = 31.27 ± 1.93 hr, ± = standard deviation, Figure 4d). In summary, these data show that expression of any of the ELF3 orthologs is sufficient to recover the amplitude and restore rhythms of the *CCA1::LUC* reporter.

3.5 | BdELF3 and SvELF3 are integrated into a similar protein-protein interaction network in *Arabidopsis*

Despite relatively low sequence conservation at the protein level, the ELF3 orthologs can complement a wide array of *elf3* phenotypes (Figures 2–4). As ELF3 functions within the evening complex (EC) in Arabidopsis, which also contains the transcription factor LUX and the DUF-1313 domain containing protein ELF4 (Herrero et al., 2012; Nusinow et al., 2011), we reasoned that the monocot *ELF3* orthologs may also be able to bind to these proteins when expressed in *Arabidopsis*. To determine whether a composite EC could be formed, we tested whether BdELF3 or SvELF3 could directly interact with AtLUX or AtELF4 in a yeast two-hybrid assay. Similar to AtELF3 (Nusinow et al., 2011), both BdELF3 and SvELF3 directly interact with both AtELF4 and the C-terminal portion of AtLUX (Figure 5). We cannot conclude that whether monocot ELF3 orthologs are also able to interact with the N-terminal AtLUX, as this fragment auto-activated the reporter gene in the yeast two-hybrid assay (Figure 5).

ELF3 functions not only as the scaffold of the EC, but also as a hub protein in a protein-protein interaction network containing multiple key regulators in both the circadian clock and light signaling

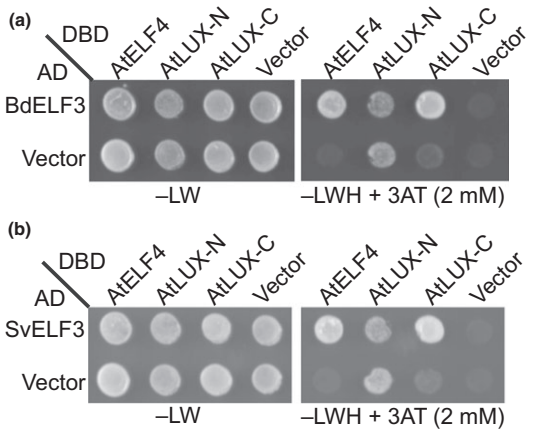

FIGURE 5 Both BdELF3 and SvELF3 can directly bind to AtELF4 and AtLUX. Yeast two-hybrid analysis of testing whether either BdELF3 (a) or SvELF3 (b) can directly interact with either AtELF4, the N-terminal half of AtLUX (AtLUX-N, a.a. 1-143) or the C-terminal half of AtLUX (AtLUX-C, a.a. 144-324). –LW tests for the presence of both bait (DBD) and pray (AD) vectors, while the –LWH + 3AT tests for interaction. Vector alone serves as interaction control. This experiment was repeated twice with similar results

pathways (Huang & Nusinow, 2016b; Huang, Alvarez, Bindbeutel, et al., 2016). We hypothesize that BdELF3 and SvELF3 could rescue many of the defects of the *elf3* mutant because both monocot versions were integrated into the same protein-protein interaction network. To test this hypothesis, we used affinity purification and mass spectrometry (AP-MS) to identify the proteins that co-precipitate with monocot ELF3s when expressed in *Arabidopsis*. AP-MS on two biological replicates for each sample with the above-mentioned independent insertion lines were included for each ELF3 ortholog. For comparison, the same AP-MS experiment was performed with one of the 35S promoter-driven AtELF3-HFC transgenic lines (AtELF3-2). To detect specific co-precipitating proteins, we manually removed commonly identified contaminant proteins from plant affinity purifications and mass spectrometry experiments (van Leene et al., 2015), and proteins identified from a control transgenic line expressing GFP-His_6-3xFlag described previously (Huang, Alvarez, Bindbeutel, et al., 2016) (Table 1, the full list of identified proteins can be found in Table S2).

We have previously reported proteins that co-precipitated with ELF3 driven from its native promoter using a similar AP-MS methodology (Huang, Alvarez, Bindbeutel, et al., 2016). When using the 35S promoter-driven AtELF3 transgenic line, we were able to generate a curated list of 22 proteins that specifically co-precipitate with AtELF3, including all previously identified proteins, such as all five phytochromes, PHOTOPERIODIC CONTROL OF HYPOCOTYL1 (PCH1) (Huang, Yoo, et al., 2016), and COP1 (Table 1). In addition, we also identified LIGHT-REGULATED WD 2 (LWD2) and SPA1-RELATED 4 (SPA4) as now co-precipitating with AtELF3. These additional interactions may be a result of a combination of altered seedling age, expression level of the ELF3 bait, or tissue-specificity of expression due to these purifications are from tissues where the epitope-tagged transgene is constitutively over-expressed. However, as LWD2 is a known component of the circadian clock (Wu, Wang, & Wu, 2008) and SPA4 is a known component of the COP1-SPA complex (Zhu et al., 2008), these interactions are likely to be relevant.

In comparing the list of BdELF3 and SvELF3 co-precipitated proteins with that of AtELF3, we found that neither SvELF3 nor BdELF3 co-precipitated SPA2 and SPA4, components of the COP1-SPA complex. In addition, SvELF3 did not co-precipitate MUT9-LIKE KINASE1, a kinase with roles in chromatin modification and circadian rhythms as AtELF3 did (Huang, Alvarez, Bindbeutel, et al., 2016; Wang et al., 2015). However, BdELF3 and SvELF3 associated with most of the proteins found in AtELF3 AP-MS (20 of 22 for BdELF3, 19 of 22 for SvELF3), in at least one of the replicate purifications from each monocot ortholog AP-MS. Therefore, our data suggest that BdELF3 and SvELF3 are integrated into a similar protein-protein interaction network as AtELF3, which likely underlies their ability of broadly complementing *elf3* mutants.

4 | DISCUSSION

Recent work in diverse plant species has found that the circadian clock plays critical roles in regulating metabolism, growth, photoperiodism, and other agriculturally important traits (Bendix, Marshall, & Harmon, 2015; McClung, 2013; Rubin et al., 2017; Shor & Green, 2016). While the relevance of the circadian clock to plant physiology is recognized, it is unclear whether the circadian clock components have conserved function among different plant species. This is particularly true for the majority of clock proteins, whose biological functions are currently poorly understood at the molecular level (Hsu & Harmer, 2014). Also, the divergent modes of growth regulation and photoperiodism between monocots and dicots suggest that the clock evolved to have altered roles in regulating these physiological responses between lineages (Matos et al., 2014; Poire et al., 2010; Song, Shim, Kinmonth-Schultz, & Imaizumi, 2014). Here, we asked whether orthologs of ELF3 from two monocots could complement any of the loss-of-function phenotypes in the model dicot plant *Arabidopsis*. In this study we found that ELF3 from either *Brachypodium* or *Setaria* could complement the hypocotyl elongation, early flowering, and arrhythmic clock phenotype of the *elf3* mutant in *Arabidopsis*, despite the variations in protein sequences and evolutionary divergence between monocot and dicot plants. These data suggest that monocot ELF3s can functionally substitute for *Arabidopsis* ELF3, albeit with varying efficacy. As monocot and dicot ELF3 are largely different in the protein sequences, functional conservation of ELF3 orthologs also leads to the next open question of identifying the functional domains within ELF3.

Previously, comparison of ELF3 homologs has identified at least five conserved regions that may be important for function (Fig. S1) (Liu et al., 2001; Saito et al., 2012; Weller et al., 2012). Our multiple sequence alignments also show that at least two regions of AtELF3, namely the N-terminus (AA 1~49) and one middle region (AA

TABLE 1 Proteins co-purified with ELF3 orthologs from AP-MS

			Exclusive unique peptide count/percent coverage[a] (%)									
			AtELF3		SvELF3 #2		SvELF3 #3		BdELF3 #2		BdELF3 #3	
AGI number	Protein name	Molecular weight	rep1	rep2	rep1	rep2	rep1	rep2	rep1	rep2	rep1	rep2
n/a	AtELF3-HFC	84 kDa	20/36	19/31	–	–	–	–	–	–	–	–
n/a	SvELF3-HFC	87 kDa	–	–	19/40	29/48	22/42	33/54	–	–	–	–
n/a	BdELF3-HFC	86 kDa	–	–	–	–	–	–	25/42	26/43	21/35	19/33
AT2G18790	phyB	129 kDa	23/37	24/37	31/54	28/42	32/50	30/45	22/34	22/33	24/40	24/37
AT5G35840	phyC	124 kDa	22/29	23/29	27/37	32/39	27/37	33/42	20/24	18/22	19/23	22/27
AT5G43630	TZP	91 kDa	14/21	12/17	13/23	20/33	13/22	24/36	12/18	13/19	14/20	14/22
AT4G18130	phyE	123 kDa	11/16	19/27	12/18	18/23	11/19	17/24	6/7	10/14	14/19	13/18
AT2G16365.2	PCH1[b]	51 kDa	9/25	9/25	9/30	14/43	11/36	16/49	9/26	9/28	11/32	11/32
AT2G46340	SPA1	115 kDa	8/14	7/9	2/2	4/8	2/3	4/9	–	–	6/8	5/6
AT3G42170[c]	DAYSLEEPER	79 kDa	8/19	5/11	–	7/16	–	12/27	3/7	4/8	2/4	–
AT2G32950	COP1	76 kDa	8/16	9/17	6/17	4/8	3/6	5/12	1/2	2/4	6/11	4/8
AT3G22380	TIC	165 kDa	5/5	5/5	4/4	12/12	3/3	15/15	4/4	3/3	1/1	1/1
AT4G11110	SPA2	115 kDa	5/11	6/12	–	–	–	–	–	–	–	–
AT2G40080	ELF4	12 kDa	4/50	4/50	3/42	5/68	4/60	4/60	4/50	4/50	5/68	5/68
AT1G09340[c]	CRB	43 kDa	4/16	3/12	1/4	1/4	1/4	4/18	1/4	1/4	–	–
AT3G13670	MLK4	79 kDa	3/10	3/13	–	–	–	1/2	6/21	3/10	3/11	5/13
AT5G61380	TOC1	69 kDa	2/4	2/4	2/5	–	3/7	–	–	–	1/2	1/2
AT1G53090	SPA4	89 kDa	2/6	5/14	–	–	–	–	–	–	–	–
AT5G18190	MLK1	77 kDa	2/12	2/11	–	–	–	–	2/14	2/14	2/11	2/11
AT3G26640	LWD2	39 kDa	2/21	1/21	–	1/16	–	2/22	3/27	1/16	–	–
AT1G12910	LWD1	39 kDa	2/21	3/30	2/21	4/31	1/17	2/21	2/22	2/19	–	–
AT4G16250	phyD	129 kDa	1/10	1/11	2/12	1/12	3/15	2/12	2/11	1/10	2/14	2/12
AT1G09570	phyA	125 kDa	1/1	1/1	7/11	5/5	7/11	2/2	–	2/2	6/7	3/4
AT2G25760	MLK3	76 kDa	1/5	1/6	–	1/4	–	1/4	3/13	2/9	2/9	2/9
AT3G03940	MLK2	78 kDa	1/8	1/8	–	1/7	–	–	3/20	2/13	3/13	1/9
AT3G46640	LUX	35 kDa	1/3	1/3	–	3/19	–	3/23	1/3	1/3	1/3	2/11
AT1G17455	ELF4-L4	13 kDa	–	–	–	–	–	–	1/23	1/23	–	–
AT1G72630	ELF4-L2	13 kDa	–	1/11	–	1/13	–	–	1/22	1/22	1/22	1/11

Proteins co-purified with ELF3 orthologs (AtELF3, SvELF3 and BdELF3, with C-terminal His_6-3xFLAG tag) were identified from affinity purification coupled with mass spectrometry (AP-MS) analyses using 12L:12D grown, 10-day-old transgenic plants (in *elf3-2 null* mutant backgrounds) harvested at ZT12.

[a]All listed proteins match 99% protein threshold, minimum number peptides of two distinct peptides across all purifications and peptide threshold as 95%. Proteins not matching the criteria were marked with "–".

[b]Percent coverage for PCH1 is calculated using protein encoded by *At2g16365.2*.

[c]These proteins have been noted as frequently identified proteins in AP-MS experiments (see van Leene et al., 2015).

317~389) share many conserved residues with ELF3 orthologs in grasses (Fig. S1). These regions fall within known fragments that are sufficient for binding to phyB (Liu et al., 2001), COP1 (Yu et al., 2008), or ELF4 (Herrero et al., 2012). Consistent with the hypothesis that these conserved regions are critical for proper ELF3 function, a single amino acid substitution (A362V) within this middle region results in defects of ELF3 nuclear localization and changes in the circadian clock period (Anwer et al., 2014). In addition, our protein–protein interaction study and AP-MS analysis show that both monocot ELF3 can form composite ECs (Figure 5) and that all three ELF3 homologs interact with an almost identical set of proteins *in vivo* (Table 1), further suggesting that one or more of the conserved regions may mediate the binding between ELF3 and its known interacting proteins. Furthermore, the similar pool of ELF3 interacting proteins identified by Bd/SvELF3 AP-MS suggests that the overall conformation of ELF3 ortholog proteins is conserved and that similar complexes and interactions with ELF3 orthologs may form in monocot species. However, whether these interactions form *in planta* and have the same effect on physiology is unclear. For example, *Setaria* data generated here and public data for *Brachypodium* and rice

showed that *ELF3* does not cycle under circadian conditions, which differs from *Arabidopsis*. Further, different from the fact that the clock plays a key role in regulating elongation in *Arabidopsis* (Nozue et al., 2007), the circadian clock has no influence on growth in C3 model grass *Brachypodium*, despite robust oscillating expression of putative clock components (Matos et al., 2014). Similarly, ELF3 from rice and soybean promotes flowering and senescence (Lu et al., 2017; Saito et al., 2012; Sakuraba, Han, Yang, Piao, & Paek, 2016; Yang, Peng, Chen, Li, & Wu, 2013; Zhao et al., 2012), while in *Arabidopsis*, ELF3 represses these responses (Liu et al., 2001; Sakuraba et al., 2014; Zagotta et al., 1992), which suggests significant rewiring of ELF3 regulated photoperiodic responses of flowering between short-day (rice/soybean) and long-day (*Arabidopsis*) plants. Alternatively, ELF3 may form distinct interactions and complexes in monocot species that were not identified in our trans-species complementation analysis. Clearly, further work is required to understand ELF3 function in monocots beyond the studies presented here.

In addition to the molecular characterization of ELF3, our analysis of circadian-regulated genes in *Setaria* after photo- and thermo-entrainment found significant differences in the behavior of the clock when compared to other monocots. Although the number of circadian-regulated genes is comparable to studies carried out in maize and rice after photo-entrainment (between 10% and 12%) (Filichkin et al., 2011; Khan et al., 2010), we found that very few genes (~1%) continue to cycle after release from temperature entrainment in *Setaria* (Fig. S4) when compared to rice (~11%) (Filichkin et al., 2011). This may reflect a fundamental difference in how the clock interfaces with temperature between these monocot species. Furthermore, proportions of circadian-regulated genes upon photo-entrainment in all three monocot plants (Fig. S4) (Filichkin et al., 2011; Khan et al., 2010) are much smaller than the approximately 30% reported for *Arabidopsis* (Covington et al., 2008), suggesting the divergence of clock functions through evolution or domestication. Further comparisons of circadian responses among monocots or between monocots and dicots will help to determine the molecular underpinning of these differences.

In summary, we find that BdELF3 and SvELF3 form similar protein complexes *in vivo* as AtELF3, which likely allows for functional complementation of loss of function of *elf3* despite relatively low sequence conservation. We also present an online query tool, Diel Explorer that allows for exploration of circadian gene expression in *Setaria*, which illustrate fundamental differences in clock function among monocots and between monocots and dicots. Collectively, this work is a first step toward functional understanding of the circadian clock in two model monocots, *Brachypodium* and *Setaria*.

ACKNOWLEDGEMENTS

We would like to thank all the funding agencies. In addition, we would like to thank the reviewers of this manuscript for the thoughtful comments that improved this work.

AUTHOR CONTRIBUTIONS

H.H., M.A.G., T.C.M., and D.A.N. conceived the project; T.C.M., B.S.E., and D.A.N. supervised the experiments; H.H., M.A.G., S.E.H., S.A., C.L., E.L.G., J.G., M.J.N., R.K.B., and D.A.N. performed the experiments; H.H., M.A.G., S.E.H., S.A., C.L., M.J.N., and D.A.N. analyzed the data; H.H., M.A.G., and D.A.N. wrote the manuscript. All authors edited the manuscript.

REFERENCES

Altschul, S. F., Gish, W., Miller, W., Myers, E. W., & Lipman, D. J. (1990). Basic local alignment search tool. *Journal of Molecular Biology*, *215*, 403–410.

Anwer, M. U., Boikoglou, E., Herrero, E., Hallstein, M., Davis, A. M., Velikkakam James, G., … Davis, S. J. (2014). Natural variation reveals that intracellular distribution of ELF3 protein is associated with function in the circadian clock. *eLife*, *3*, e02206.

Barrett, T., Wilhite, S. E., Ledoux, P., Evangelista, C., Kim, I. F., Tomashevsky, M., … Soboleva, A. (2013). NCBI GEO: archive for functional genomics data sets–update. *Nucleic Acids Research*, *41*, D991–D995.

Bell-Pedersen, D., Cassone, V. M., Earnest, D. J., Golden, S. S., Hardin, P. E., Thomas, T. L., & Zoran, M. J. (2005). Circadian rhythms from multiple oscillators: Lessons from diverse organisms. *Nature Reviews Genetics*, *6*, 544–556.

Bendix, C., Marshall, C. M., & Harmon, F. G. (2015). Circadian clock genes universally control key agricultural traits. *Molecular Plant*, *8*, 1135–1152.

Bennetzen, J. L., Schmutz, J., Wang, H., Percifield, R., Hawkins, J., Pontaroli, A. C., … Devos, K. M. (2012). Reference genome sequence of the model plant Setaria. *Nature Biotechnology*, *30*, 555–561.

Boikoglou, E., Ma, Z., von Korff, M., Davis, A. M., Nagy, F., & Davis, S. J. (2011). Environmental memory from a circadian oscillator: The Arabidopsis thaliana clock differentially integrates perception of photic vs. thermal entrainment. *Genetics*, *189*, 655–664.

Bray, N. L., Pimentel, H., Melsted, P., & Pachter, L. (2016). Near-optimal probabilistic RNA-seq quantification. *Nature Biotechnology*, *34*, 525–527.

Brutnell, T. P., Wang, L., Swartwood, K., Goldschmidt, A., Jackson, D., Zhu, X. G., … van Eck, J. (2010). Setaria viridis: A model for C4 photosynthesis. *Plant Cell*, *22*, 2537–2544.

Bushnell, B. (2016). BBMap short read aligner. *University of California, Berkeley, California*. URL http://sourceforge. net/projects/bbmap.

Calixto, C. P., Waugh, R., & Brown, J. W. (2015). Evolutionary relationships among barley and Arabidopsis core circadian clock and clock-associated genes. *Journal of Molecular Evolution*, *80*, 108–119.

Covington, M. F., Maloof, J. N., Straume, M., Kay, S. A., & Harmer, S. L. (2008). Global transcriptome analysis reveals circadian regulation of key pathways in plant growth and development. *Genome Biology*, *9*, R130.

Covington, M. F., Panda, S., Liu, X. L., Strayer, C. A., Wagner, D. R., & Kay, S. A. (2001). ELF3 modulates resetting of the circadian clock in Arabidopsis. *Plant Cell*, *13*, 1305–1315.

Dixon, L. E., Knox, K., Kozma-Bognar, L., Southern, M. M., Pokhilko, A., & Millar, A. J. (2011). Temporal repression of core circadian genes is mediated through EARLY FLOWERING 3 in Arabidopsis. *Current Biology*, *21*, 120–125.

Dodd, A. N., Salathia, N., Hall, A., Kevei, E., Toth, R., Nagy, F., … Webb, A. A. (2005). Plant circadian clocks increase photosynthesis, growth, survival, and competitive advantage. *Science*, *309*, 630–633.

Doherty, C. J., & Kay, S. A. (2010). Circadian control of global gene expression patterns. *Annual Review of Genetics*, *44*, 419–444.

Doyle, M. R., Davis, S. J., Bastow, R. M., McWatters, H. G., Kozma-Bognar, L., Nagy, F., ... Amasino, R. M. (2002). The ELF4 gene controls circadian rhythms and flowering time in Arabidopsis thaliana. *Nature*, *419*, 74–77.

Edelstein, A., Amodaj, N., Hoover, K., Vale, R., & Stuurman, N. (2010). Computer control of microscopes using microManager. *Current Protocols in Molecular Biology*, *14*(Unit14), 20.

Edelstein, A. D., Tsuchida, M. A., Amodaj, N., Pinkard, H., Vale, R. D., & Stuurman, N. (2014). Advanced methods of microscope control using muManager software. *Journal of Biological Methods*, *1*.

Edgar, R., Domrachev, M., & Lash, A. E. (2002). Gene Expression Omnibus: NCBI gene expression and hybridization array data repository. *Nucleic Acids Research*, *30*, 207–210.

Edgar, R. S., Green, E. W., Zhao, Y., van Ooijen, G., Olmedo, M., Qin, X., ... Reddy, A. B. (2012). Peroxiredoxins are conserved markers of circadian rhythms. *Nature*, *485*, 459–464.

Faure, S., Turner, A. S., Gruszka, D., Christodoulou, V., Davis, S. J., von Korff, M., & Laurie, D. A. (2012). Mutation at the circadian clock gene EARLY MATURITY 8 adapts domesticated barley (*Hordeum vulgare*) to short growing seasons. *Proceedings of the National Academy of Sciences*, *109*, 8328–8333.

Filichkin, S. A., Breton, G., Priest, H. D., Dharmawardhana, P., Jaiswal, P., Fox, S. E., ... Mockler, T. C. (2011). Global profiling of rice and poplar transcriptomes highlights key conserved circadian-controlled pathways and cis-regulatory modules. *PLoS ONE*, *6*, e16907.

Goodstein, D. M., Shu, S., Howson, R., Neupane, R., Hayes, R. D., Fazo, J., ... Rokhsar, D. S. (2012). Phytozome: A comparative platform for green plant genomics. *Nucleic Acids Research*, *40*, D1178–D1186.

Gould, P. D., Diaz, P., Hogben, C., Kusakina, J., Salem, R., Hartwell, J., & Hall, A. (2009). Delayed fluorescence as a universal tool for the measurement of circadian rhythms in higher plants. *Plant Journal*, *58*, 893–901.

Graf, A., Schlereth, A., Stitt, M., & Smith, A. M. (2010). Circadian control of carbohydrate availability for growth in Arabidopsis plants at night. *Proceedings of the National Academy of Sciences*, *107*, 9458–9463.

Green, R. M., Tingay, S., Wang, Z. Y., & Tobin, E. M. (2002). Circadian rhythms confer a higher level of fitness to Arabidopsis plants. *Plant Physiology*, *129*, 576–584.

Greenham, K., & McClung, C. R. (2015). Integrating circadian dynamics with physiological processes in plants. *Nature Reviews Genetics*, *16*, 598–610.

Harmer, S. L. (2009). The circadian system in higher plants. *Annual Review of Plant Biology*, *60*, 357–377.

Harmer, S. L., Hogenesch, J. B., Straume, M., Chang, H. S., Han, B., Zhu, T., ... Kay, S. A. (2000). Orchestrated transcription of key pathways in Arabidopsis by the circadian clock. *Science*, *290*, 2110–2113.

Hazen, S. P., Schultz, T. F., Pruneda-Paz, J. L., Borevitz, J. O., Ecker, J. R., & Kay, S. A. (2005). LUX ARRHYTHMO encodes a Myb domain protein essential for circadian rhythms. *Proceedings of the National Academy of Sciences*, *102*, 10387–10392.

Helfer, A., Nusinow, D. A., Chow, B. Y., Gehrke, A. R., Bulyk, M. L., & Kay, S. A. (2011). LUX ARRHYTHMO encodes a nighttime repressor of circadian gene expression in the Arabidopsis core clock. *Current Biology*, *21*, 126–133.

Herrero, E., Kolmos, E., Bujdoso, N., Yuan, Y., Wang, M., Berns, M. C., ... Davis, S. J. (2012). EARLY FLOWERING4 recruitment of EARLY FLOWERING3 in the nucleus sustains the Arabidopsis circadian clock. *Plant Cell*, *24*, 428–443.

Hicks, K. A., Albertson, T. M., & Wagner, D. R. (2001). EARLY FLOWERING3 encodes a novel protein that regulates circadian clock function and flowering in Arabidopsis. *Plant Cell*, *13*, 1281–1292.

Hicks, K. A., Millar, A. J., Carre, I. A., Somers, D. E., Straume, M., Meeks-Wagner, D. R., & Kay, S. A. (1996). Conditional circadian dysfunction of the Arabidopsis early-flowering 3 mutant. *Science*, *274*, 790–792.

Higgins, J. A., Bailey, P. C., & Laurie, D. A. (2010). Comparative genomics of flowering time pathways using Brachypodium distachyon as a model for the temperate grasses. *PLoS ONE*, *5*, e10065.

Hsu, P. Y., & Harmer, S. L. (2014). Wheels within wheels: The plant circadian system. *Trends in Plant Science*, *19*, 240–249.

Huang, H., Alvarez, S., Bindbeutel, R., Shen, Z., Naldrett, M. J., Evans, B. S., ... Nusinow, D. A. (2016). Identification of evening complex associated proteins in arabidopsis by affinity purification and mass spectrometry. *Molecular & Cellular Proteomics: MCP*, *15*, 201–217.

Huang, H., Alvarez, S., & Nusinow, D. A. (2016). Data on the identification of protein interactors with the Evening Complex and PCH1 in Arabidopsis using tandem affinity purification and mass spectrometry (TAP-MS). *Data Brief*, *8*, 56–60.

Huang, H., & Nusinow, D. (2016a). Tandem purification of His_6-3x FLAG tagged proteins for mass spectrometry from arabidopsis. *Bio-Protocol*, *6*.

Huang, H., & Nusinow, D. A. (2016b). Into the evening: complex interactions in the arabidopsis circadian clock. *Trends in Genetics*, *32*, 674–686.

Huang, H., Yoo, C. Y., Bindbeutel, R., Goldsworthy, J., Tielking, A., Alvarez, S., ... Nusinow, D. A. (2016). CH1 integrates circadian and light-signaling pathways to control photoperiod-responsive growth in Arabidopsis. *eLife*, *5*, e13292.

Hughes, M. E., Hogenesch, J. B., & Kornacker, K. (2010). JTK_CYCLE: An efficient nonparametric algorithm for detecting rhythmic components in genome-scale data sets. *Journal of Biological Rhythms*, *25*, 372–380.

Keller, A., Nesvizhskii, A. I., Kolker, E., & Aebersold, R. (2002). Empirical statistical model to estimate the accuracy of peptide identifications made by MS/MS and database search. *Analytical Chemistry*, *74*, 5383–5392.

Khan, S., Rowe, S. C., & Harmon, F. G. (2010). Coordination of the maize transcriptome by a conserved circadian clock. *BMC Plant Biology*, *10*, 126.

Khanna, R., Kikis, E. A., & Quail, P. H. (2003). EARLY FLOWERING 4 functions in phytochrome B-regulated seedling de-etiolation. *Plant Physiology*, *133*, 1530–1538.

Kim, W. Y., Hicks, K. A., & Somers, D. E. (2005). Independent roles for EARLY FLOWERING 3 and ZEITLUPE in the control of circadian timing, hypocotyl length, and flowering time. *Plant Physiology*, *139*, 1557–1569.

Kolmos, E., Herrero, E., Bujdoso, N., Millar, A. J., Toth, R., Gyula, P., ... Davis, S. J. (2011). A reduced-function allele reveals that EARLY FLOWERING3 repressive action on the circadian clock is modulated by phytochrome signals in Arabidopsis. *Plant Cell*, *23*, 3230–3246.

Kumar, R., Ichihashi, Y., Kimura, S., Chitwood, D. H., Headland, L. R., Peng, J., ... Sinha, N. R. (2012). A high-throughput method for illumina RNA-Seq library preparation. *Frontiers in Plant Science*, *3*, 202.

van Leene, J., Eeckhout, D., Cannoot, B., de Winne, N., Persiau, G., van de Slijke, E., ... de Jaeger, G. (2015). An improved toolbox to unravel the plant cellular machinery by tandem affinity purification of Arabidopsis protein complexes. *Nature Protocols*, *10*, 169–187.

Li, P., Ponnala, L., Gandotra, N., Wang, L., Si, Y., Tausta, S. L., ... Brutnell, T. P. (2010). The developmental dynamics of the maize leaf transcriptome. *Nature Genetics*, *42*, 1060–1067.

Liu, X. L., Covington, M. F., Fankhauser, C., Chory, J., & Wagner, D. R. (2001). ELF3 encodes a circadian clock-regulated nuclear protein that functions in an Arabidopsis PHYB signal transduction pathway. *Plant Cell*, *13*, 1293–1304.

Lou, P., Wu, J., Cheng, F., Cressman, L. G., Wang, X., & McClung, C. R. (2012). Preferential retention of circadian clock genes during diploidization following whole genome triplication in *Brassica rapa*. *Plant Cell*, *24*, 2415–2426.

Lu, S., Zhao, X., Hu, Y., Liu, S., Nan, H., Li, X., ... Kong, F. (2017). Natural variation at the soybean J locus improves adaptation to the tropics and enhances yield. *Nature Genetics*, *49*, 773–779.

Matos, D. A., Cole, B. J., Whitney, I. P., Mackinnon, K. J., Kay, S. A., & Hazen, S. P. (2014). Daily changes in temperature, not the circadian clock, regulate growth rate in Brachypodium distachyon. *PLoS ONE*, *9*, e100072.

Matsubara, K., Ogiso-Tanaka, E., Hori, K., Ebana, K., Ando, T., & Yano, M. (2012). Natural variation in Hd17, a homolog of Arabidopsis ELF3 that is involved in rice photoperiodic flowering. *Plant and Cell Physiology*, *53*, 709–716.

McClung, C. R. (2013). Beyond Arabidopsis: The circadian clock in non-model plant species. *Seminars in Cell & Developmental Biology*, *24*, 430–436.

Michael, T. P., Mockler, T. C., Breton, G., Mcentee, C., & Byer, A. (2008). Network discovery pipeline elucidates conserved time-of-day-specific cis-regulatory modules. *PLoS Genetics*, *4*, e14.

Michael, T. P., Salome, P. A., & McClung, C. R. (2003). Two Arabidopsis circadian oscillators can be distinguished by differential temperature sensitivity. *Proceedings of the National Academy of Sciences*, *100*, 6878–6883.

Mizuno, T., Nomoto, Y., Oka, H., Kitayama, M., Takeuchi, A., Tsubouchi, M., & Yamashino, T. (2014). Ambient temperature signal feeds into the circadian clock transcriptional circuitry through the EC night-time repressor in *Arabidopsis thaliana*. *Plant and Cell Physiology*, *55*, 958–976.

Mockler, T. C., Michael, T. P., Priest, H. D., Shen, R., Sullivan, C. M., Givan, S. A., … Chory, J. (2007). The DIURNAL project: DIURNAL and circadian expression profiling, model-based pattern matching, and promoter analysis. *Cold Spring Harbor Symposia on Quantitative Biology*, *72*, 353–363.

Murakami, M., Ashikari, M., Miura, K., Yamashino, T., & Mizuno, T. (2003). The evolutionarily conserved OsPRR quintet: Rice pseudo-response regulators implicated in circadian rhythm. *Plant and Cell Physiology*, *44*, 1229–1236.

Nagel, D. H., & Kay, S. A. (2012). Complexity in the wiring and regulation of plant circadian networks. *Current Biology*, *22*, R648–R657.

Nesvizhskii, A. I., Keller, A., Kolker, E., & Aebersold, R. (2003). A statistical model for identifying proteins by tandem mass spectrometry. *Analytical Chemistry*, *75*, 4646–4658.

Nozue, K., Covington, M. F., Duek, P. D., Lorrain, S., Fankhauser, C., Harmer, S. L., & Maloof, J. N. (2007). Rhythmic growth explained by coincidence between internal and external cues. *Nature*, *448*, 358–361.

Nusinow, D. A., Helfer, A., Hamilton, E. E., King, J. J., Imaizumi, T., Schultz, T. F., … Kay, S. A. (2011). The ELF4-ELF3-LUX complex links the circadian clock to diurnal control of hypocotyl growth. *Nature*, *475*, 398–402.

Onai, K., & Ishiura, M. (2005). PHYTOCLOCK 1 encoding a novel GARP protein essential for the Arabidopsis circadian clock. *Genes to Cells*, *10*, 963–972.

Ouyang, Y., Andersson, C. R., Kondo, T., Golden, S. S., & Johnson, C. H. (1998). Resonating circadian clocks enhance fitness in cyanobacteria. *Proceedings of the National Academy of Sciences*, *95*, 8660–8664.

Plautz, J. D., Straume, M., Stanewsky, R., Jamison, C. F., Brandes, C., Dowse, H. B., … Kay, S. A. (1997). Quantitative analysis of drosophila period gene transcription in living animals. *Journal of Biological Rhythms*, *12*, 204–217.

Poire, R., Wiese-Klinkenberg, A., Parent, B., Mielewczik, M., Schurr, U., Tardieu, F., & Walter, A. (2010). Diel time-courses of leaf growth in monocot and dicot species: Endogenous rhythms and temperature effects. *Journal of Experimental Botany*, *61*, 1751–1759.

Pokhilko, A., Fernandez, A. P., Edwards, K. D., Southern, M. M., Halliday, K. J., & Millar, A. J. (2012). The clock gene circuit in Arabidopsis includes a repressilator with additional feedback loops. *Molecular Systems Biology*, *8*, 574.

Pruneda-Paz, J. L., Breton, G., Para, A., & Kay, S. A. (2009). A functional genomics approach reveals CHE as a component of the Arabidopsis circadian clock. *Science*, *323*, 1481–1485.

Rubin, M. J., Brock, M. T., Davis, A. M., German, Z. M., Knapp, M., Welch, S. M., … Weinig, C. (2017). Circadian rhythms vary over the growing season and correlate with fitness components. *Molecular Ecology*.

Saito, H., Ogiso-Tanaka, E., Okumoto, Y., Yoshitake, Y., Izumi, H., Yokoo, T., … Tanisaka, T. (2012). Ef7 encodes an ELF3-like protein and promotes rice flowering by negatively regulating the floral repressor gene Ghd7 under both short- and long-day conditions. *Plant and Cell Physiology*, *53*, 717–728.

Sakuraba, Y., Han, S. H., Yang, H. J., Piao, W., & Paek, N. C. (2016). Mutation of rice early flowering3.1 (OsELF3.1) delays leaf senescence in rice. *Plant Molecular Biology*, *92*, 223–234.

Sakuraba, Y., Jeong, J., Kang, M. Y., Kim, J., Paek, N. C., & Choi, G. (2014). Phytochrome-interacting transcription factors PIF4 and PIF5 induce leaf senescence in Arabidopsis. *Nature Communications*, *5*, 4636.

Schneider, C. A., Rasband, W. S., & Eliceiri, K. W. (2012). NIH Image to ImageJ: 25 years of image analysis. *Nature Methods*, *9*, 671–675.

Shor, E., & Green, R. M. (2016). The impact of domestication on the circadian clock. *Trends in Plant Science*, *21*, 281–283.

Sievers, F., Wilm, A., Dineen, D., Gibson, T. J., Karplus, K., Li, W., … Higgins, D. G. (2011). Fast, scalable generation of high-quality protein multiple sequence alignments using Clustal Omega. *Molecular Systems Biology*, *7*, 539.

Song, Y. H., Ito, S., & Imaizumi, T. (2010). Similarities in the circadian clock and photoperiodism in plants. *Current Opinion in Plant Biology*, *13*, 594–603.

Song, Y. H., Shim, J. S., Kinmonth-Schultz, H. A., & Imaizumi, T. (2014). Photoperiodic flowering: Time measurement mechanisms in leaves. *Annual Review of Plant Biology*, *66*, 441–464.

Vizcaino, J. A., Deutsch, E. W., Wang, R., Csordas, A., Reisinger, F., Rios, D., … Hermjakob, H. (2014). ProteomeXchange provides globally coordinated proteomics data submission and dissemination. *Nature Biotechnology*, *32*, 223–226.

Wang, W., Barnaby, J. Y., Tada, Y., Li, H., Tor, M., Caldelari, D., … Dong, X. (2011). Timing of plant immune responses by a central circadian regulator. *Nature*, *470*, 110–114.

Wang, Z., Casas-Mollano, J. A., Xu, J., Riethoven, J. J., Zhang, C., & Cerutti, H. (2015). Osmotic stress induces phosphorylation of histone H3 at threonine 3 in pericentromeric regions of Arabidopsis thaliana. *Proceedings of the National Academy of Sciences*, *112*, 8487–8492.

Wang, L., Czedik-Eysenberg, A., Mertz, R. A., Si, Y., Tohge, T., Nunes-Nesi, A., … Brutnell, T. P. (2014). Comparative analyses of C4 and C3 photosynthesis in developing leaves of maize and rice. *Nature Biotechnology*, *32*, 1158–1165.

Wang, L., Si, Y., Dedow, L. K., Shao, Y., Liu, P., & Brutnell, T. P. (2011). A low-cost library construction protocol and data analysis pipeline for Illumina-based strand-specific multiplex RNA-seq. *PLoS ONE*, *6*, e26426.

Weller, J. L., Liew, L. C., Hecht, V. F. G., Rajandran, V., Laurie, R. E., Ridge, S., … Lejeune-Hénaut, I. (2012). A conserved molecular basis for photoperiod adaptation in two temperate legumes. *Proceedings of the National Academy of Sciences*, *109*, 21158–21163.

Wijnen, H., & Young, M. W. (2006). Interplay of circadian clocks and metabolic rhythms. *Annual Review of Genetics*, *40*, 409–448.

Woelfle, M. A., Ouyang, Y., Phanvijhitsiri, K., & Johnson, C. H. (2004). The adaptive value of circadian clocks: An experimental assessment in cyanobacteria. *Current Biology*, *14*, 1481–1486.

Wu, J. F., Wang, Y., & Wu, S. H. (2008). Two new clock proteins, LWD1 and LWD2, regulate Arabidopsis photoperiodic flowering. *Plant Physiology*, *148*, 948–959.

Yang, Y., Peng, Q., Chen, G.-X., Li, X.-H., & Wu, C.-Y. (2013). OsELF3 is involved in circadian clock regulation for promoting flowering under long-day conditions in rice. *Molecular Plant*, *6*, 202–215.

Yu, J. W., Rubio, V., Lee, N. Y., Bai, S., Lee, S. Y., Kim, S. S., … Deng, X. W. (2008). COP1 and ELF3 control circadian function and photoperiodic flowering by regulating GI stability. *Molecular Cell*, *32*, 617–630.

Zagotta, M., Shannon, S., Jacobs, C., & Meeks-Wagner, D. (1992). Early-flowering mutants of *Arabidopsis thaliana*. *Functional Plant Biology*, *19*, 411–418.

Zakhrabekova, S., Gough, S. P., Braumann, I., Muller, A. H., Lundqvist, J., Ahmann, K., … Hansson, M. (2012). Induced mutations in circadian clock regulator Mat-a facilitated short-season adaptation and range extension in cultivated barley. *Proceedings of the National Academy of Sciences*, *109*, 4326–4331.

Zhang, X., Henriques, R., Lin, S.-S., Niu, Q.-W., & Chua, N.-H. (2006). Agrobacterium-mediated transformation of Arabidopsis thaliana using the floral dip method. *Nature Protocols*, *1*, 641–646.

Zhao, J., Huang, X., Ouyang, X., Chen, W., Du, A., Zhu, L., … Li, S. (2012). OsELF3-1, an ortholog of Arabidopsis early flowering 3, regulates rice circadian rhythm and photoperiodic flowering. *PLoS ONE*, *7*, e43705.

Zhu, D., Maier, A., Lee, J. H., Laubinger, S., Saijo, Y., Wang, H., … Deng, X. W. (2008). Biochemical characterization of Arabidopsis complexes containing CONSTITUTIVELY PHOTOMORPHOGENIC1 and SUPPRESSOR OF PHYA proteins in light control of plant development. *Plant Cell*, *20*, 2307–2323.

SUPPORTING INFORMATION

Additional Supporting Information may be found online in the supporting information tab for this article.

How to cite this article: Huang H, Gehan MA, Huss SE, et al. Cross-species complementation reveals conserved functions for EARLY FLOWERING 3 between monocots and dicots. *Plant Direct*. 2017;00:1–14. https://doi.org/10.1002/pld3.18